COMMUNICATION

ChemComm
www.rsc.org/chemcomm

# A building block approach to the synthesis of organic–inorganic oxide materials: the hydrothermal synthesis and network structure of $[\{Ni_4(tpypyz)_3\}\{Mo_5O_{15}(O_3PCH_2CH_2PO_3)\}_2]\cdot 23H_2O$ (tpypyz = tetra-2-pyridylpyrazine)

**Eric Burkholder,[a] Vladimir Golub,[b] Charles J. O'Connor[b] and Jon Zubieta*[a]**

[a] *Department of Chemistry, Syracuse University, Syracuse, NY 13244, USA. E-mail: jazubiet@syr.edu*

[b] *Department of Chemistry, University of New Orleans, New Orleans, LA, USA*

*Received (in Cambridge, UK) 1st April 2003, Accepted 15th July 2003*

*First published as an Advance Article on the web 24th July 2003*

**The hydrothermal reaction of $MoO_3$, $[Ni(CH_3CO_2)_2]\cdot 4H_2O$, tpypyz, ethylenediphosphonic acid and water yields the 2D material $[\{Ni_4(tpypyz)_3\}\{Mo_5O_{15}(O_3PCH_2CH_2PO_3)\}_2]\cdot 23H_2O$ (1·23$H_2O$), constructed from $\{Mo_5O_{15}(O_3PCH_2CH_2PO_3)\}^{4-}$ clusters linked in one-dimension through the ethylene tethers of the diphosphonate component; these molybdodiphosphonate chains are in turn linked into a 2D network through the tetranuclear secondary metal–ligand subunit $\{Ni_4(tpypyz)_3\}^{8+}$.**

Although inorganic oxides represent an ubiquitous class of materials characterized by a vast compositional range and considerable structural versatility, and exhibiting useful electronic, magnetic, optical and mechanical properties for functional materials construction,[1,2] their synthesis by rational design remains elusive.[3] One synthetic strategy exploits molecular building blocks in the form of chemically robust polyoxoanions linked through direct condensation or through secondary metal–ligand coordination complexes acting as inorganic bridging subunits.[4–8] In our variant of this approach, the well known molybdophosphonate clusters[9] of the type $[Mo_5O_{15}(O_3PR)_2]^{4-}$ are linked into one-dimensional organic/inorganic oxides through the straightforward expedient of tethering the organophosphonate components through appropriate organic spacers. However, it is noteworthy that the syntheses of the target chains of linked clusters required the presence of secondary metal–ligand subunits as charge compensating and surface passivating components.[10] This three component system of oxide cluster, organic tether and secondary metal–ligand complex[11] could be exploited in turn to expand the dimensionality of the hybrid oxide product by using a binucleating ligand to allow propagation in a second dimension (Scheme 1). Characteristic one- and two-dimensional materials include $[\{Cu(bpy)_2\}\{Cu(bipy)(H_2O)\}(Mo_5O_{15})\{O_3P(CH_2)_4PO_3\}]$ and $[\{Cu_2(tpypyz)(H_2O)_2\}(Mo_5O_{15})(O_3PCH_2CH_2PO_3)]$, respectively. To date, some thirty compounds of the three component system molybdenum oxide/$O_3$E-linker-$EO_3$/Cu-organonitrogen have been isolated.[10–12] The structures reflect the size of the molybdate cluster and the number and accessibility of attachment points for linkers, the electronic and geometric constraints of the organic tethers and the coordination flexibility of the Cu(II) site. However, the coordination preferences of the Jahn–Teller $d^9$ Cu(II) component, which adopts '4 + 1' and '4 + 2' geometries in most instances, are quite distinct from those of Co(II) or Ni(II) which favor more regular octahedral geometry. In an attempt to define the structural consequences of introducing a secondary metal component other than Cu(II), we have begun to explore the phosphomolybdate/Ni(II)-organonitrogen ligand system, which has yielded the expected two-dimensional material with an unanticipated architecture, $[\{Ni_4(tpypyz)_3\}\{Mo_5O_{15}(O_3PCH_2CH_2PO_3)\}_2]\cdot 23H_2O$ (**1**·23$H_2O$).

† Electronic supplementary information (ESI) available: crystal data tables. See http://www.rsc.org/suppdata/cc/b3/b303659f/

Compound **1** was produced in 25% yield as orange crystals in the hydrothermal reaction of $MoO_3$, $[Ni(CH_3CO_2)_2]\cdot 4H_2O$, ethylenediphosphonic acid and hydrofluoric acid (48–51%).‡ The infrared spectrum of **1** exhibited a strong band at 918 $cm^{-1}$ attributed to $\nu$(Mo=O) and a group of three medium to strong intensity bands between 1046 and 1129 $cm^{-1}$ associated with $\nu$(P–O) of the diphosphonate component.

As shown in Fig. 1, the structure of **1**§ consists of one-dimensional $\{Mo_5O_{15}(O_3PCH_2CH_2PO_3)\}_n^{4n-}$ chains linked through unprecedented $\{Ni_4(tpypyz)_3\}^{8+}$ chains into a two-dimensional network. While the molybdophosphonate chain of **1** is identical to that observed for $[\{Cu_2(tpypyz)(H_2O)_2\}Mo_5O_{15}(O_3PCH_2CH_2PO_3)]$, which is constructed from $\{Mo_5O_{21}\}$ cyclic clusters tethered through diphosphonate ligands, the secondary metal–ligand subunits linking the chains into the network architecture are quite distinct. The Cu analogue exhibits the anticipated binuclear subunit $\{Cu_2(tpypyz)(H_2O)_2\}^{4+}$, bridging adjacent molybdophosphonate chains

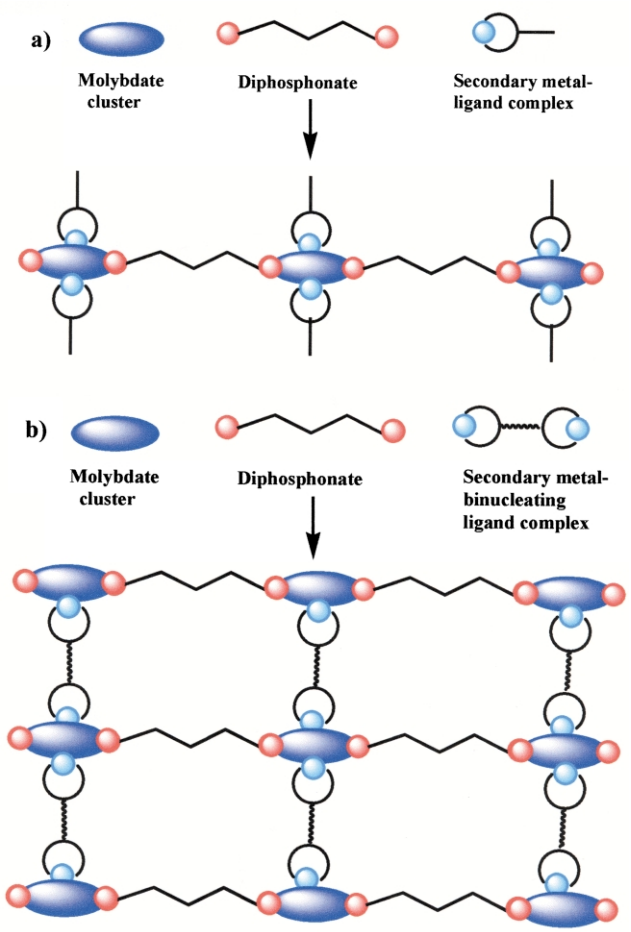


**Scheme 1**

DOI: 10.1039/b303659f

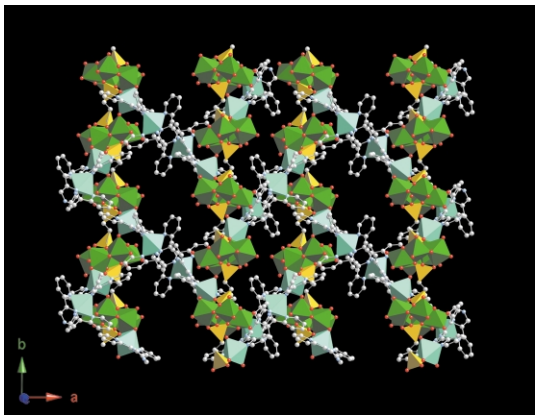

**Fig. 1** A polyhedral representation of the 2-D structure of **1**·23$H_2O$ in the *ab* plane. Molybdenum octahedra: green; nickel octahedra: blue; carbon: light gray spheres; oxygen: red spheres; nitrogen: blue spheres; phosphorus, yellow tetrahedra.

to produce an interchain spacing of 14.7 Å within the network. In contrast, the coordination polymer bridge of **1** is the tetranuclear unit $\{Ni_4(tpypyz)_3\}^{8+}$ which results in an interchain spacing of 24.5 Å. One consequence of the expansion of the secondary metal–ligand building block is to produce an intralamellar cavity of dimensions *ca*. 9.6 × 19.3 Å, which can accommodate a significant number of water molecules of crystallization, *ca*. 22.8 $H_2O$ per cavity.

The disposition of the secondary metal–ligand subunits with respect to the molybdophosphonate chains produces a distinct ruffling of the network, such that the view of the layer parallel to the crystallographic *b* axis (Fig. 2) reveals the sinusoidal profile with a period of 24.7 Å and an amplitude of 16.0 Å.

The tetranuclear $\{Ni_4(tpypyz)_3\}^{8+}$ subunit exhibits two distinct Ni(II) environments. The terminal Ni(II) sites display $\{NiO_3N_3\}$ geometry through coordination to three nitrogen donors of the tpypyz ligand, two terminal oxo-groups {Mo=O} of two adjacent clusters of the molybdophosphonate chain and a phosphonate {P–O–Mo} oxygen atom. Thus, this Ni(II) center shares an edge with an Mo site of one cluster and a vertex with a site on the adjacent cluster. The two interior Ni(II) sites display $\{NiN_6\}$ geometry through bonding to three nitrogen donors from each of two tpypyz ligands. Consequently, two tpypyz units bridge terminal and interior Ni(II) sites, while the third bridges the two interior Ni(II) centers of the chain.

The magnetic susceptibility of **1**·23$H_2O$ as a function of temperature shows a maximum at *ca*. 14 K, indicative of antiferromagnetic interactions. The experimental results were

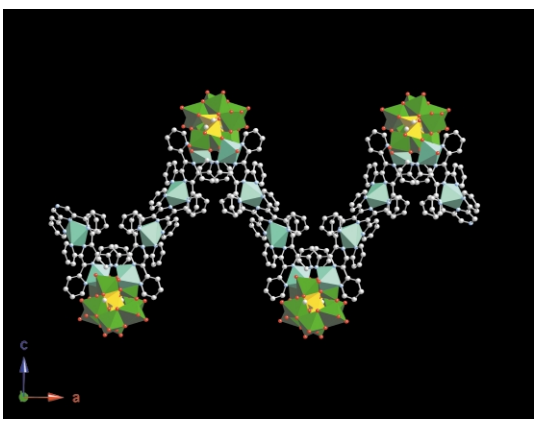

**Fig. 2** A view of the structure of **1**·23$H_2O$ parallel to the crystallographic *b* axis, showing the ruffling of the network.

fit to the linear Heisenberg tetramer model ($S$ = 1) with the Hamiltonian:

$$\mathscr{H} = -2J(S_1 \cdot S_2 + S_2 \cdot S_3 + S_3 \cdot S_4) - g\mu_B H \cdot \sum_{i=1}^{4} S_i$$

The best fit was consistent with $g$ = 2.01, $J$ = −7.0 K, TIP = −0.00073 and an intertetramer exchange $zJ$ = 2.3 K.

At 300 K, the measured $\mu_{eff}$ is 5.84 $\mu_B$ per $Ni_4$ unit while the theoretical value for four Ni(II) sites in octahedral environments ($S$ = 1) is 5.66 $\mu_B$. The larger value of the measured $\mu_{eff}$ is ascribed to orbital contributions. The value of $\mu_{eff}$ does not change significantly with lowering temperature until 50 K where it begins to drop precipitously to 0.70 $\mu_B$ at 2.5 K.

The thermal decomposition of **1**·23$H_2O$ exhibits a dehydration process from just above room temperature to *ca*. 100 °C resulting in an 8% weight loss, consistent with the loss of 16 water molecules of crystallization. There is a second dehydration process between 400–500 °C accounting for *ca*. 4% weight loss associated with the remaining water molecules. A weight loss of *ca*. 30% at 600 °C is consistent with loss of the organic component. The resulting gray powder is amorphous and could not be identified. However, the product of the initial dehydration process exhibited an X-ray powder pattern nearly identical to that of the parent compound. The sorptive properties of this material are under investigation.

This work was supported by a grant from the National Science Foundation (CHE0242153).

## Notes and references

‡ *Synthesis*.The reaction of $MoO_3$ (0.160 g, 1.112 mmol), $[Ni(CH_3CO_2)_2]\cdot 4H_2O$ (0.110 g, 0.442 mmol), tpyprz (0.086 g, 0.221 mmol), $H_2PO_3(CH_2)_2PO_3H_2$ (0.084 g, 0.442 mmol), $H_2O$ (10.03 g, 557 mmol) and HF (48–51%, 0.123 g) in the mole ratio 5.03 : 2.00 : 1.00 : 2.00 : 2520 at 200 °C for 96 h yielded orange crystals of **1**·22.8$H_2O$ in 25% yield based on Mo which were suitable for X-ray diffraction. Initial pH: 1.5; final pH, 1.0.

§ *Crystal data*: **1**·23$H_2O$, $C_{38}N_9H_{51}Mo_5O_{32.5}Ni_2P_2$, orthorhombic *Pbca*, $a$ = 24.674(1), $b$ = 15.4148(8), $c$ = 30.813(2) Å, $V$ = 11719(1) Å$^3$, $Z$ = 8, $D_{calc}$ = 2.053 g cm$^{-3}$; $R1$ = 0.072, $wR2$ = 0.1179 for 21129 reflections. While the water molecules of crystallization exhibit some disorder, the total water content is confirmed by thermal gravimetric analysis. The magnetic data were recorded on a 13.42 mg polycrystalline sample of **1**·23$H_2O$ in the 2–300 K temperature range, using a Quantum Design MPMS-SS SQUID spectrometer. The temperature dependent magnetic data were obtained at a magnetic field of $H$ = 1000 Oe. CCDC reference number 205940. See http://www.rsc.org/suppdata/cc/b3/b303659f/ for crystallographic data in .cif or other electronic format.


1 N. N. Greenwood and A. Earnshaw, *Chemistry of the Elements*, Pergamon Press, New York 1984.
2 W. H. McCarroll, *Oxides: Solid State Chemistry*, in *Encyclopedia of Inorganic Chemistry*, ed. R. B. King; John Wiley & Sons, NY, **vol. 6**, p. 2903.
3 A. Stein, S. Keller and T. E. Mallouk, *Science*, 1993, **259**, 1558.
4 J. R. D. DeBord, R. C. Haushalter, L. M. Meyer, D. J. Rose, P. J. Zapf and J. Zubieta, *Inorg. Chim. Acta*, 1997, **256**, 165.
5 D. Hagrman, P. Hagrman and J. Zubieta, *Inorg. Chim. Acta*, 2000, **300–302**, 212 and references therein.
6 B. Yan, Y. Xu, X. Bu, N. K. Goh, L. S. Chia and G. D. Stucky, *J. Chem. Soc., Dalton Trans.*, 2001, 2009 and references therein.
7 P. J. Zapf, C. J. Warren, R. C. Haushalter and J. Zubieta, *Chem. Commun.*, 1997, 1543.
8 A. Müller, M. Koop, P. Schiffels and H. Bögge, *Chem. Commun.*, 1997, 1715.
9 W. Kwak, M. T. Pope and T. F. Scully, *J. Am. Chem. Soc.*, 1975, **97**, 5735.
10 R. C. Finn, R. S. Rarig and J. Zubieta, *Inorg. Chem.*, 2002, **41**, 2109.
11 R. C. Finn, E. Burkholder and J. Zubieta, *Chem. Commun.*, 2001, 1852.
12 E. Burkholder, V. Golub, C. J. O'Connor and J. Zubieta, *Inorg. Chem.*, 2003, **42**, in press.